Framework polymorphism and modular crystal structures of uranyl vanadates of divalent cations: synthesis and characterization of $M(UO_2)(V_2O_7)$ (M = Ca, Sr) and $Sr_3(UO_2)(V_2O_7)_2$

Saehwa Chong,[a] Sergey M. Aksenov,*[a] Fabrice Dal Bo,[a] Samuel N. Perry,[a] Foteini Dimakopoulou,[a] and Peter C. Burns [a,b]

Abstract: Uranyl vanadate compounds with divalent cations, $M(UO_2)(V_2O_7)$ (M = Ca, Sr) and $Sr_3(UO_2)(V_2O_7)_2$, were synthesized by flux crystal growth, and their crystal structures were solved using single-crystal X-ray diffraction data. $Ca(UO_2)V_2O_7$ and $Sr(UO_2)V_2O_7$ were synthesized from reactants with molar ratios M:U:V of 1:1:2 and identical heating conditions, and increasing the M:U:V ratio to 3:1:4 resulted in $Sr_3(UO_2)(V_2O_7)_2$. Crystallographic data for $M(UO_2)V_2O_7$ compounds are: a = 7.1774(18) Å, b = 6.7753(17) Å, c = 8.308(2) Å; V = 404.01(18) Å^3; sp. gr. $Pmn2_1$, Z = 2 for Ca; a = 13.4816(11) Å, b = 7.3218(6) Å, c = 8.4886(7) Å; V = 837.91(12) Å^3; sp. gr. $Pnma$, Z = 4 for Sr. Compound $Sr_3(UO_2)(V_2O_7)_2$ has a = 6.891(3) Å, b = 7.171(3) Å, c = 14.696(6) Å, α = 85.201(4)˚, β = 78.003(4)˚, γ = 89.188(4)˚; V = 707.9(5) Å^3; sp. gr. P-1, Z = 2. The framework structure of $Sr(UO_2)(V_2O_7)$ is related to that of $Pb(UO_2)(V_2O_7)$ reported previously, while that of $Ca(UO_2)(V_2O_7)$ has a different topology. The topological polymorphism of the $[(UO_2)(V_2O_7)]$-type framework may be due to the differing ionic radii of the guest M^{2+} cations. Compound $Sr_3(UO_2)(V_2O_7)_2$ has a modular structure based on two different types of electroneutral layers: $[Sr(UO_2)(V_2O_7)]$ and $[Sr_2(V_2O_7)]$. Structural complexities were calculated, and Raman spectra were collected and their peaks were assigned.

Introduction

Uranium production in the USA peaked between the 1940s and 1980s during operation of thousands of uranium mines mostly in the western United States, leaving abandoned mines with potential hazards to the environment and humans.[1] Uranium reacts with hydroxide, carbonate, or alkaline earth metals in oxidizing conditions affecting the mobility of uranium in water.[2-4] Uranium and vanadium species can form solid phases including vanadate, phosphate, silicate, and carbonate minerals.[5-8] Uraninite (UO_{2+x}), davidite [$La(Y,U)Fe_2(Ti,Fe,Cr,V)_{18}(O,OH,F)_{38}$], and montroseite [$(V^{3+},V^{4+},Fe^{2+})O(OH)$] are major minerals that can alter to form uranyl vanadate minerals.[9,10] Studies of the crystal chemistry and various properties of uranium-containing minerals and compounds are helpful for understanding the influence of radionuclides on human health and the environment.[3,11-13]

Carnotite-group minerals are uranyl vanadates with a layer structure[9] that are commonly found in abandoned mine sites in the U.S. Southwest, and experiments indicate that these minerals can be formed by precipitation reactions of uranium and vanadium precursors.[7,14,15] Various carnotite analogues have been studied with the general chemical formula $M_x(UO_2)_2V_2O_8{\cdot}nH_2O$ (M = Na, K, Rb, Cs, Tl, Ag for x = 2 and M = Ca, Cu, Pb, Ni, Ln^{3+} for x = 1; n = 0–8.5), $(Na_{1-x}K_x)_2(UO_2)_2V_2O_8$ ($0 \le x \le 1$), and $Al(UO_2)_2V_2O_8(OH){\cdot}8.5H_2O$.[16-24] The carnotite family is characterized by francevillite-type $[(UO_2)_2V_2O_8]^{2-}$ sheets formed by $[V_2O_8]^{6-}$ units and $(UO_2)^{2+}$ ions. The $[V_2O_8]^{6-}$ unit is formed by two inversely symmetric VO_5 square pyramids sharing an edge of their bases, and another edge is shared between the square base and a uranyl pentagonal bipyramid formed by five equatorial oxygen atoms around the $(UO_2)^{2+}$ ion. Cations with oxidation states ranging from +1 to +3 are located in the interlayer space between the $[(UO_2)_2V_2O_8]^{2-}$ sheets.

In addition to minerals and compounds with the francevillite sheet-anion topology, VO_5 square pyramids also occur in $Cs(UO_2)V_3O_9$.[25] The structure of $Cs(UO_2)V_3O_9$ contains $[(UO_2)_2V_3O_9]^-$ sheets formed by corner-sharing VO_5 square pyramids and by UO_8 hexagonal bipyramids in the spaces within the array of VO_5 polyhedra. A similar layered structure is also found in UV_3O_{10}, and a study of cation exchange in related $M(UO_2)V_3O_9{\cdot}nH_2O$ (M = Na, Mg, NH_4, or H_3O) compounds has been reported.[26]

Uranyl vanadates with VO_4 tetrahedra are also reported.[27-32] $M_6(UO_2)_5(VO_4)_2O_5$ (M = Na, K, Rb) has $[(UO_2)_5(VO_4)_2O_5]^{6-}$ corrugated layers formed by UO_7 pentagonal bipyramids, UO_6 octahedra, and VO_4 tetrahedra.[27,28] $(UO_2)_3(VO_4)_2{\cdot}5H_2O$ has a framework formed by $[(UO_2)VO_4]^-$ layers connected by $(UO_2)^{2+}$ ions and water molecules.[29]

Finally, $(UO_2)_2(V_2O_7)$, $Cs_4(UO_2)_2(V_2O_7)O_2$, and $Pb(UO_2)(V_2O_7)$ have pyrovanadate V_2O_7 units formed by two VO_4 tetrahedra the share one of their oxygen atoms.[30-33] $(UO_2)_2(V_2O_7)$ contains corrugated chains of UO_7 uranyl pentagonal bipyramids connected by V_2O_7 units. $Cs_4(UO_2)_2(V_2O_7)O_2$ has $[(UO_2)_2(V_2O_7)O_2]^{4-}$ corrugated layers formed by UO_6 octahedra and V_2O_7 units, whereas $Pb(UO_2)(V_2O_7)$ has a framework structure formed by chains of

[a] Dr. Saehwa Chong, Dr. Sergey M. Aksenov, Dr. Fabrice Dal Bo, B.Sc. Samuel N. Perry, B.Sc. Foteini Dimakopoulou, Prof. Dr. Peter C. Burns
Department of Civil and Environmental Engineering and Earth Sciences
University of Notre Dame
Notre Dame, Indiana 46556, United States
E-mail: aks.crys@gmail.com

[b] Prof. Dr. Peter C. Burns
Department of Chemistry and Biochemistry
University of Notre Dame
Notre Dame, Indiana 46556, United States

Supporting information for this article is given via a link at the end of the document.

WILEY-VCH

alternating U and Pb pentagonal bipyramids connected by V_2O_7 units by sharing their corners.

The present work continues our crystal chemical study of alkaline and alkaline-earth uranyl vanadates[34] and further develops understanding of uranyl-based frameworks.[35] Here we report the flux synthesis[36] and crystal structures of the new uranyl vanadates $M(UO_2)V_2O_7$ (M = Ca, Sr) and $Sr_3(UO_2)(V_2O_7)_2$ with a framework and a layer-type structure, respectively. Raman spectra, sheet-anion topologies, and structural complexities are discussed.

Results and Discussion

Synthesis

Caution! *The uranium compounds used in these studies contained depleted uranium salts that are radioactive. Precautions were performed for handling radioactive materials, and all studies were conducted in a laboratory dedicated to studies of actinide elements by properly trained individuals and with institutional oversight.*

Single crystals of $M(UO_2)V_2O_7$ (M = Ca, Sr) were obtained by mixing 0.35 mmol of $UO_2(NO_3)_2{\cdot}6H_2O$ with a calcium/strontium nitrate and vanadium oxide in the M:U:V (M = Ca, Sr) molar ratio of 1:1:2 and Sr:U:V molar ratio of 3:1:4. The precursors were homogeneously mixed with ethanol using a mortar and pestle. The mixtures were dried at room temperature, heated to 870˚C in a porcelain crucible and dwelled for 5 h, cooled to 370˚C at 5˚C/h, and furnace-cooled to room temperature. The products were washed using an ultrasonic bath and vacuum filtration with water.

The products from the reactions consisted of yellow-green crystals for $M(UO_2)V_2O_7$ (M = Ca, Sr) and $Sr_3(UO_2)(V_2O_7)_2$ as shown in Fig. S1. Crystals were synthesized along with yellow (M = Ca) and black and yellow (M = Sr) X-ray amorphous powders. Mixture of precursors with the molar ratio M:U:V = 1:1:2 resulted in $M(UO_2)V_2O_7$. The same heating conditions but molar ratio Sr:U:V = 3:1:4 resulted in $Sr_3(UO_2)(V_2O_7)_2$. Increasing the concentration of Sr in the precursor mixture crystalized the compound with a higher Sr:U ratio; however, no Ca-analogue was crystalized under the same conditions.

Vibrational spectra

Raman spectra of $M(UO_2)V_2O_7$ (M = Ca, Sr) and $Sr_3(UO_2)(V_2O_7)_2$ at room temperature are shown in Fig. 1. The Raman spectra of all three compounds are similar due to the similarities in their structures composed of UO_7 pentagonal bipyramids and V_2O_7 pyrovanadate groups. The intense bands observed at 773, 787, and 785 cm^{-1} are assigned to symmetric stretching vibrations of $(UO_2)^{2+}$ uranyl ions for $Ca(UO_2)V_2O_7$, $Sr(UO_2)V_2O_7$, and $Sr_3(UO_2)(V_2O_7)_2$ respectively.[37,38] For all three compounds, the bands between 247 and 285 cm^{-1} are assigned to bending vibrations of $(UO_2)^{2+}$ uranyl ions.[38] The bands from 852 to 914 are assigned to antisymmetric stretching vibrations of $(UO_2)^{2+}$ uranyl ions;[37,38] however, other studies suggests these bands are due to stretching vibrations of VO_3.[39,40]. The vibrations from the equatorial U-O bonds are in the range from 450 to 552 cm^{-1}.[41a] The bands from 335 to 400, 697 to 755, and 922 to 961 are assigned to bending vibrations of VO_3, antisymmetric stretching of V-O-V and VO_3, and symmetric stretching mode of VO_3 respectively.[38-40,41b] Detailed assignments of all the peaks are summarized in Table S1.

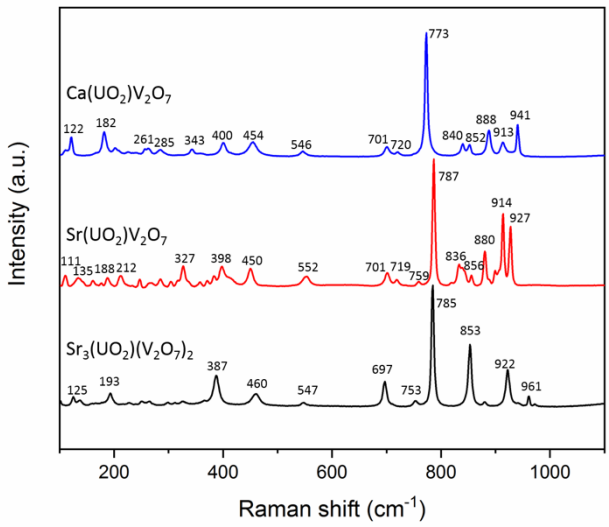

Figure 1. Raman spectra of $Ca(UO_2)(V_2O_7)$, $Sr(UO_2)(V_2O_7)$, and $Sr_3(UO_2)(V_2O_7)_2$.

Crystal structures

Cation coordination: In all the structures uranium forms nearly linear $(UO_2)^{2+}$ uranyl (Ur) ions that are surrounded by five equatorial oxygen atoms (U_{eq}). The average U-O_{yl} and U-O_{eq} bond lengths in these UrO_5 pentagonal bipyramids vary from 1.782 to 1.806 Å and from 2.351 to 2.374 Å, respectively, which are in good agreement with reported values.[42,43] Vanadium forms distorted tetrahedra that are linked to form V_2O_7 diortho-vanadate groups. Each VO_4 tetrahedron has three V–O distances that vary from 1.627 to 1.723 Å, as well as an elongated distance to the bridging oxygens (O_{br}) between two VO_4 tetrahedra with V–O_{br} ranging from 1.759 to 1.846 Å. The value of the V-O-V angle depends on the alkaline-earth cation incorporated into the crystal structure and varies from 131.1 to 139.1°. Alkaline-earth cations are coordinated in polyhedra with high coordination numbers: CaO_7 (<Ca-O> = 2.428 Å) and SrO_{7-9} (<Sr-O> = 2.428 to 2.677 Å).

Crystal structures and topology of $M(UO_2)(V_2O_7)$ (M = Ca, Sr): The crystal structures of $Ca(UO_2)(V_2O_7)$ and $Sr(UO_2)(V_2O_7)$ (Fig. 2) have a microporous heteropolyhedral framework that is similar to that in the structure of $Pb(UO_2)(V_2O_7)$[33] (Fig. 3) and that is based on isolated UrO_5 uranyl pentagonal bipyramids linked together by V_2O_7 pyrovanadate groups with the ratio UrO_5 : V_2O_7 = 1 : 1. The cavities of the frameworks are filled by the large divalent cations (Ca^{2+}, Sr^{2+}, Pb^{2+}).

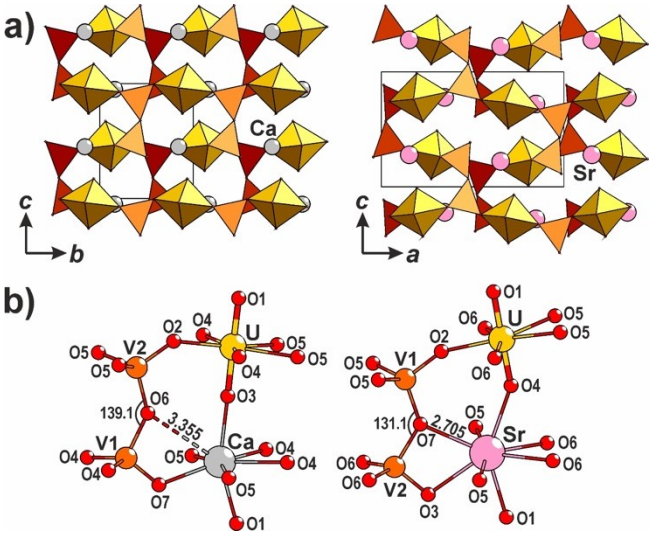

Figure 2. Heteropolyhedral frameworks in the crystal structures of $Ca(UO_2)(V_2O_7)$ and $Sr(UO_2)(V_2O_7)$ (a) and the local coordination environments of the alkaline-earth elements (b). Yellow and orange polyhedra are occupied by uranium and vanadium respectively.

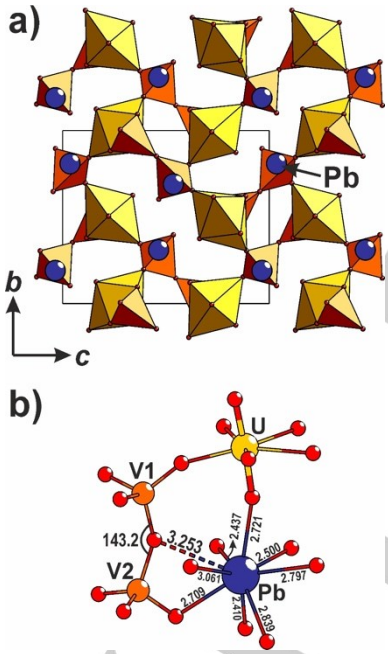

Figure 3. Heteropolyhedral frameworks in the crystal structures of $Pb(UO_2)(V_2O_7)$ (ICSD 150381) (a) and the local coordination environment of Pb (b). Yellow and orange polyhedra are occupied by uranium and vanadium respectively.

Topological analysis based on natural tiling analysis of the 3D cation nets[44] can be useful to characterize heteropolyhedral frameworks[45-48] and was recently applied for the analysis of uranyl germanates.[35] The ToposPro software[49] was used for the topological calculations. The framework in the structure of $Sr(UO_2)(V_2O_7)$ is related to that of $Pb(UO_2)(V_2O_7)$ (Fig. 4) and is characterized by the following set of natural tiles: $[6^2.8^2][8^2.10^2]$. The framework in the structure of $Ca(UO_2)(V_2O_7)$ belongs to another topological type (Fig. 5): $[8^3]_2[8^4]$.

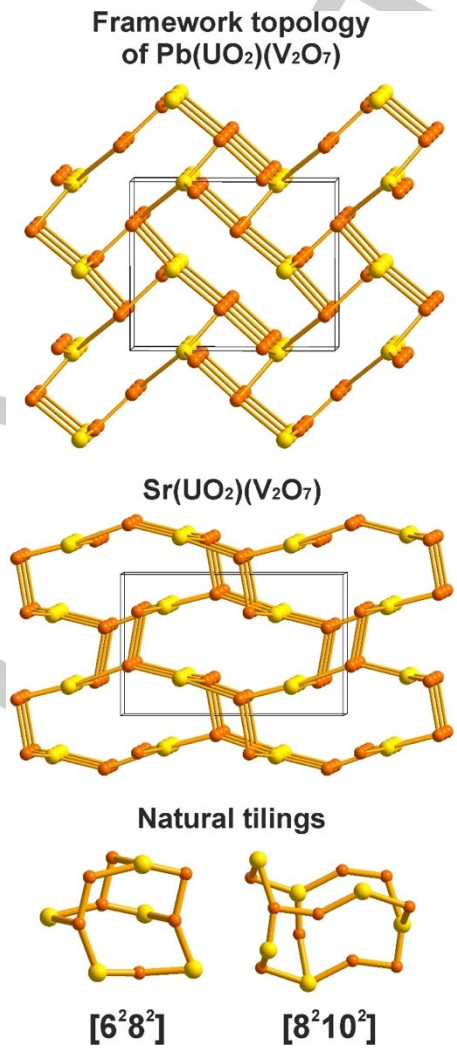

Figure 4. 3D net representation and list of natural tilings in the structures of Pb(UO2)(V2O7) and Sr(UO2)(V2O7).

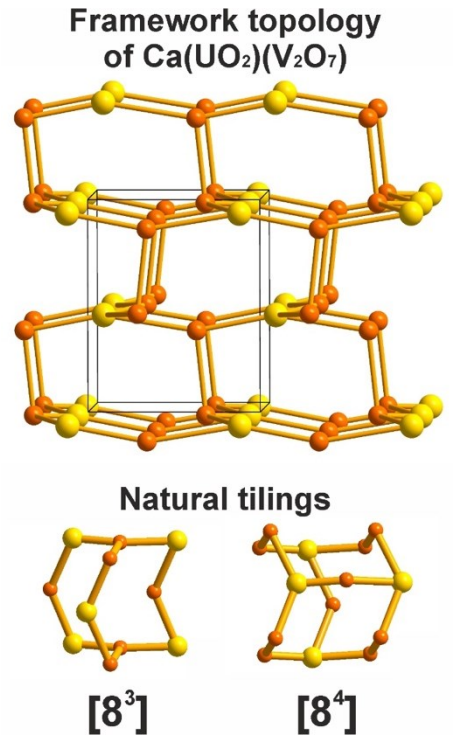

Figure 5. 3D net representation and list of natural tilings in the structure of $Ca(UO_2)(V_2O_7)$.

The topological polymorphism of the $[(U^{[5]}O_2)(V^{[4]}{}_2O_7)]^{2-}$-type framework and its distortion could result from the difference ionic radii of the M^{2+} cations incorporated into the cavities: rCa^{2+} ~ 1.12-1.18 Å, rPb^{2+} ~ 1.23-1.29 Å, and rSr^{2+} ~ 1.26-1.31 Å depending on the coordination number.[50] Comparative data for the frameworks are given in Table 1.

Table 1. Comparative data for selected uranyl-vanadate frameworks.

Parameter	Type of framework $M^{2+}[(UO_2)(V_2O_7)]$		
	Type **I**	Type **II**	
Compound	M = Ca	*M* = Pb[33]	*M* = Sr
Unit cell parameters (Å)	*a* = 7.177 *b* = 6.775 *c* = 8.308	*a* = 6.921 *b* = 9.652 *c* = 11.788 β = 91.74	*a* = 13.482 *b* = 7.322 *c* = 8.489
Volume (Å3)	404.01	787.15	837.91
Space group	$Pmn2_1$	$P2_1/n$	*Pnma*
Natural tiles	$[8^3]_2[8^4]$	$[6^2.8^2][8^2.10^2]$	
v (atoms)	10	20	
I_G (bits/atoms)	9.510	19.020	
$I_{G,total}$ (bits/unit cell)	35.020	70.039	

Modular crystal structure of $Sr_3(UO_2)(V_2O_7)_2$: Compound $Sr_3(UO_2)(V_2O_7)_2$ with the ratio UrO_5 : V_2O_7 = 1 : 2 has a layered crystal structure based on two different types of modules (Fig. 6) and can be described in terms of modular crystallography.[51,52] Module **I** with composition $Sr(UO_2)(V_2O_7)$ is a uranyl pyrovanadate double heteropolyhedral layer in which the voids are filled by Sr atoms. Along [001] module **I** alternates with uranium-free module **II**. Module **II** has composition $Sr_2(V_2O_7)$ and contains only isolated V_2O_7 pyrovanadate groups linked by Sr atoms. Module **I** is chemically related to part of the structure of $Sr(UO_2)(V_2O_7)$ (Fig. 2b), but differs in the orientation of the V_2O_7 pyrovanadate groups, whereas module **II** corresponds to part of the structure of $Sr_2(V_2O_7)$ (Fig. S2).[53]

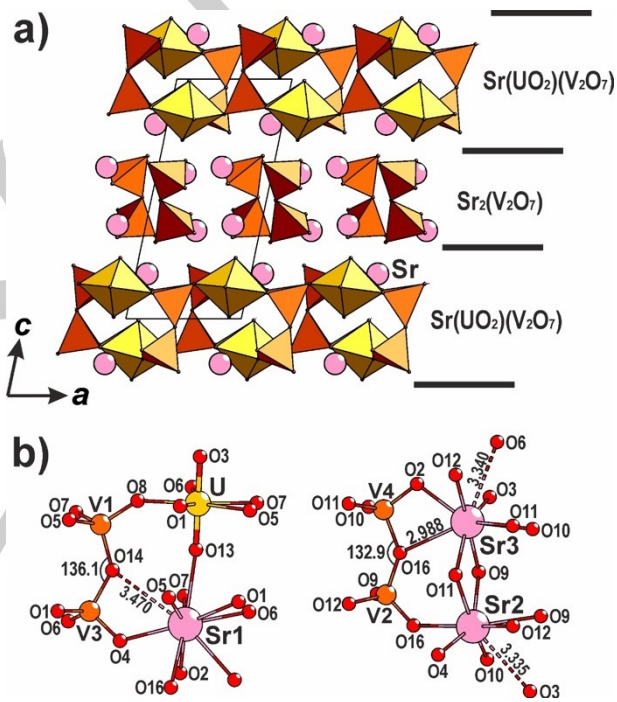

Figure 6. Modular structure of $Sr_3(UO_2)(V_2O_7)_2$ containing two modules (a), and depiction of the local coordination environment of Sr cations (b). Yellow and orange polyhedra are occupied by uranium and vanadium respectively.

Increasing of the amount of large alkaline-earth cations to the ratio Sr : U = 3 : 1 in the system (preserving the ratio $(M^{2+}+U)$: (V_2O_7) = 2 : 1) leads to formation of a differentiated structure with two kinds of modules. The detailed crystal chemical formula of $Sr_3(UO_2)(V_2O_7)_2$ is $[Sr(UO_2)(V_2O_7)]\cdot[Sr_2(V_2O_7)]$, where square brackets denote the composition of different modules.

The structure of $La(UO_2)_2(VO_4)(V_2O_7)$[54] contains a layer with composition $[La(UO_2)(V_2O_7)]^+$ that is topologically equivalent to module **I** found here (Fig. 7), where it alternates with a single uranophane-type sheet with composition $[(UO_2)(VO_4)]^-$. The combination of double and single uranophane-type layers may

be facilitated by the heterovalent substitution of alkaline-earth cations by trivalent rare-earth cations within module **I**.

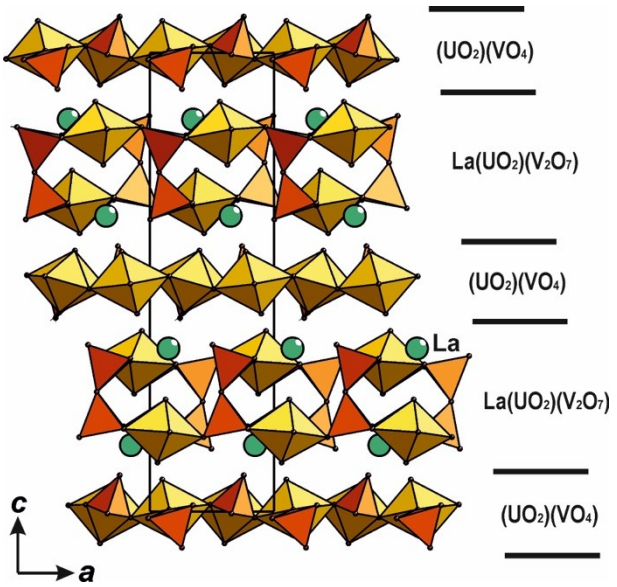

Figure 7. Modular structure of $La(UO_2)_2(VO_4)(V_2O_7)_2$ (ICSD 262324) containing two modules. Yellow and orange polyhedra are occupied by uranium and vanadium respectively.

Uranophane-type anion topology: Using the method of describing anion topologies developed by Burns et al.,[43] the anion topology of the sheet in the crystal structures of the novel compounds reported herein can be described as an array of triangles, squares and pentagons, typical of the uranophane-type topology. The uranophane sheet anion topology contains triangles (*Tr*), squares (*Sq*) and pentagons (*Pt*) in the ratio *Tr*:*Sq*:*Pt* = 1:1:1 (Fig 8a). In the corresponding sheet, pentagons are occupied by $(UO_2)^{2+}$ uranyl ions and are linked together into a chain. Adjacent chains are linked through TO_4 tetrahedra (where *T* – Si, As, P, V, Cr). These tetrahedra exhibit different orientations of their apical vertices relative to the plane of the sheet, thus forming several distinct geometrical isomers.[55] To date, roughly thirty inorganic uranyl compounds are known to have the uranophane anion-topology, and they are divided into several stereoisomers according to the orientation of the tetrahedra relative to the topological plane.[9,43,56]

In the case of $M(UO_2)V_2O_7$ (*M* = Ca, Sr) and $Sr_3(UO_2)(V_2O_7)_2$, 50% of the $(UO_2)^{2+}$ ions of the uranophane-type sheet are substituted by M^{2+} cations (*M* = Ca, Sr, Pb), forming a layer similar to that observed in the structure of ulrichite, $Cu[Ca(UO_2)(PO_4)_2](H_2O)_5$[57] and its synthetic analogs.[58] Stated differently, population of the pentagons within the chains of edge-sharing pentagons of the uranophane anion topology alternates between uranyl ions and divalent cations in the compounds studied here. Despite having the uranophane-type topology, the studied compounds belong to two different isomers (Fig. 8b-d), differing in the orientation [up (**U**) or down (**D**)] of the non-bridging oxygen of the VO4 tetrahedra. In the structure of $Ca(UO_2)V_2O_7$ the orientations of tetrahedra within the pentagonal-triangular (*PT*) chain are *UUU* for [*Ur*(VO_4)] and *DDD* for [Ca(VO_4)] chains, whereas the square-triangular (*ST*) chain sequence is *UDUD* (Fig. 8b). In the structure of $Sr(UO_2)V_2O_7$, the *PT* sequence is *UDU* for both [Ur(VO_4)] and [Sr(VO_4)] chains, but the *ST* sequences are of two different types: *UUUU* and *DDDD* (Fig. 8c). In module **I** of the structure of $Sr_3(UO_2)(V_2O_7)_2$, the sequences of both *PT* and *ST* chains are *UUUU* (Fig. 8d). The *ST* and *PT* sequences of $Ca(UO_2)V_2O_7$ are the same as in uranophane-α, boltwoodite, cuprosklodowskite, sklodowskite, and kasolite,[56] whereas the *ST* and *PT* sequences of $Sr(UO_2)V_2O_7$ are the same as the neptunyl phosphate $Rb_2[Ca(Np^{5+}O_2)_2(PO_4)_2]$.[59] Module **I** of $Sr_3(UO_2)(V_2O_7)_2$ and $La(UO_2)_2(VO_4)(V_2O_7)$[54] shows *ST* and *PT* sequences that have not been reported for any inorganic compound, and therefore corresponds to a new stereoisomer for the uranophane-anion topology.

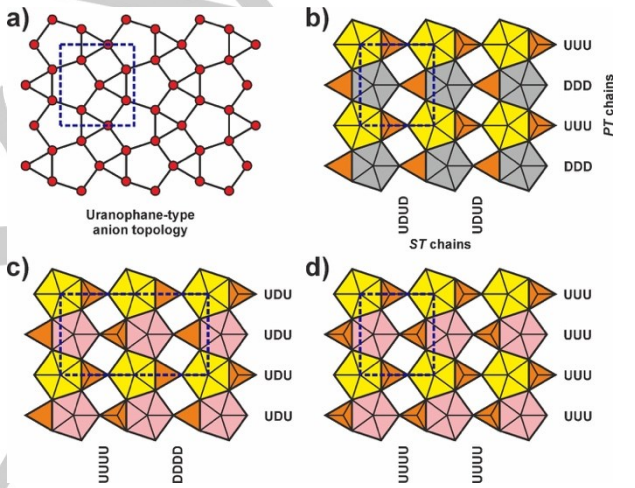

Figure 8. Uranophane type anion topology (a) and geometrical isomers in the structures of $Ca(UO_2)(V_2O_7)$ (b), $Sr(UO_2)(V_2O_7)$ (c), and $Sr_3(UO_2)(V_2O_7)_2$ (d). Yellow, gray, pink, and orange polyhedra are occupied by uranium, calcium, strontium, and vanadium respectively.

Structural complexity: Structural complexity parameters of $M(UO_2)V_2O_7$ (*M* = Ca, Sr) and $Sr_3(UO_2)(V_2O_7)_2$ were calculated using the approach of Krivovichev[60,61] using the ToposPro software.[49] The calculated values of I_G and $I_{G,total}$ are 3.393 bits/atoms and 88.211 bits/unit cell for $Ca(UO_2)(V_2O_7)$, 3.393 bits/atoms and 176.423 bits/unit cell for $Sr(UO_2)(V_2O_7)$, and 4.585 bits/atoms and 220.078 bits/unit cell for $Sr_3(UO_2)(V_2O_7)_2$. Based on the complexity classification (considering the value of $I_{G,total}$) compound $Ca(UO_2)(V_2O_7)$ has a simple structure, while compounds $Sr(UO_2)V_2O_7$ and $Sr_3(UO_2)(V_2O_7)_2$ have intermediate structures.[61] The structural complexity of $Ca(UO_2)V_2O_7$ is similar to that of carnotite-group minerals.[34] $Sr(UO_2)V_2O_7$ and $Sr_3(UO_2)(V_2O_7)_2$ have more complex structures than carnotite but less than metatyuyamunite or vanuralite.[24]

Conclusions

The framework uranyl vanadate compounds $M(UO_2)(V_2O_7)$ (M = Ca, Sr) were synthesized by flux crystal growth. The framework in the structure of $Sr(UO_2)(V_2O_7)$ is related to that in the structure of $Pb(UO_2)(V_2O_7)$, whereas the framework in the structure of $Ca(UO_2)(V_2O_7)$ belongs to another topological type. Such topological polymorphism of the framework may result from the difference of the ionic radii of the M^{2+} cations. Increasing the molar ratio of Sr:U:V from 1:1:2 to 3:1:4 in reactants with the same heating conditions led to formation of the layered compound $Sr_3(UO_2)(V_2O_7)_2$ with a modular structure based on two different types of neutral layers: $[Sr(UO_2)(V_2O_7)]\cdot[Sr_2(V_2O_7)]$.

Experimental Section

Reagents and chemicals: The following starting material were used as-received: Ca(NO3)2·4H2O (Alfa Aesar, ≥99%), Sr(NO3)2 (Alfa Aesar, 99.99%), UO2(NO3)2·6H2O (International Bio-Analytical Industries, ≥98%), and V2O5 (Alfa Aesar, 99.6%).

SEM and EDS: Scanning electron microscope (SEM) micrographs and energy dispersive spectroscopy (EDS) data were obtained using a JEOL JCM-6000 Plus microscope system. The secondary electron and backscattered electron detector were used with an acceleration voltage of 15 kV for SEM and EDS respectively. EDS spectra of the studied crystals are shown in Fig. S3. The EDS analyses were consistent with the chemical compositions deduced from the crystal structure determination.

Raman spectroscopy: Raman spectroscopy was performed on selected single crystals using a Renishaw inVia Raman microscope system. Raman spectra were obtained with a 785 nm laser at a resolution of 0.08 cm^{-1} in the range of 100-1100 cm^{-1}.

Single crystal X-ray analysis: Suitable crystals for single-crystal X-ray diffraction (SXRD) were placed on cryoloops in oil and mounted on a Bruker Quasar diffractometer with a microfocus Mo-K_α X-ray tube and an APEX II CCD detector. Data were collected with 0.5° frame widths in ω and 30 seconds dwelling per frame with the crystal held at 180 K. The Bruker APEX II software was used for determining the unit cell and integrating the data, as well as for calculating corrections for background, Lorentz, and polarization effects. Absorption corrections were done using SADABS.[62,63] Crystallographic data for $M(UO_2)V_2O_7$ compounds are: a = 7.1774(18) Å, b = 6.7753(17) Å, c = 8.308(2) Å; V = 404.01(18) Å^3; sp. gr. $Pmn2_1$, Z = 2 for Ca; a = 13.4816(11) Å, b = 7.3218(6) Å, c = 8.4886(7) Å; V = 837.91(12) Å^3; sp. gr. $Pnma$, Z = 4 for Sr. Compound $Sr_3(UO_2)(V_2O_7)_2$ has a = 6.891(3) Å, b = 7.171(3) Å, c = 14.696(6) Å, α = 85.201(4)˚, β = 78.003(4)˚, γ = 89.188(4)˚; V = 707.9(5) Å^3; sp. gr. P-1, Z = 2. Compound $Ca(UO_2)(V_2O_7)$ is a twin with a twin law [-1 0 0 / 0 1 0 / 0 0 -1] and twin ratio 0.794(8):0.206(8). Structure models were determined by the "charge flipping" method using the SUPERFLIP computer program[64] and were refined using the Jana2006 computer program.[65] Illustrations were produced using the JANA2006 program package in combination with the programs VESTA 3[66] and DIAMOND 3.[67] The final refinement cycles converged with R_1 = 0.014, 0.012, and 0.023 for $Ca(UO_2)V_2O_7$, $Sr(UO_2)V_2O_7$, and $Sr_3(UO_2)(V_2O_7)_2$ respectively. Crystallographic data and structural refinement parameters are given in Table S2. Tables S3-5 list fractional site coordinates and equivalent displacement parameters for **1** to **3**. Tables S6-8 show the anisotropic displacement parameters. Selected bond distances are given in Tables S9–11. CCDC 1896438–1896440 contain the supplementary crystallographic data for these compounds. The data can be obtained free of charge from The Cambridge Crystallographic Data Centre via www.ccdc.cam.ac.uk/structures. Bond valence sum (BVS) calculations (Table S12-S14) were performed using parameters for U^{6+}–O,[68] and V^{5+}–O, Ca^{2+}–O, Sr^{2+}–O.[69] The BVS results confirmed the oxidation states for U(VI) and V(V).

Acknowledgments

This research was funded by the U.S. Department of Energy, National Nuclear Security Administration, under Award Number DE-NA0003763.

Keywords: uranyl vanadates • topology • modularity • flux crystal growth • structural complexity

[1] U.S. EPA, *Uranium Location Database Compilation*, U.S. Environmental Protection Agency, Washington, DC, **2006**.
[2] N.P. Qafoku, J.M. Zachara, C. Liu, P.L. Gassman, O.S. Qafoku, S.C. Smith, *Environ. Sci. Technol.* **2005**, 39, 3157-3165.
[3] S. Avasarala, P.C. Lichtner, A.-M.S. Ali, R. González-Pinzón, J.M. Blake, J.M. Cerrato, *Environ. Sci. Technol.* **2017**, 51, 12385-12393.
[4] W. Dong, S.C. Brooks, *Environ. Sci. Technol.* **2006**, 40, 4689-4695.
[5] R. Bernier-Latmani, H. Veeramani, E.D. Vecchia, P. Junier, J.S. Lezama-Pacheco, E.I. Suvorova, J.O. Sharp, N.S. Wigginton, J. Bargar, *Environ. Sci. Technol.* **2010**, 44, 9456-9462.
[6] P.L. Hansley, C.S. Spirakis, *Econ. Geol.* **1992**, 87, 352-365.
[7] T.K. Tokunaga, Y. Kim, J. Wan, *Environ. Sci. Technol.* **2009**, 43, 5467-5471.
[8] T.L. Spano, E.A. Dzik, M. Sharifironizi, M.K. Dustin, M. Turner, P.C. Burns, *Am. Mineral.* **2017**, 102, 1149-1153.
[9] S.V. Krivovichev, J. Plášil, in *Uranium: Cradle to Grave* (Eds.: P.C. Burns, G.E. Sigmon), Mineralogical Association of Canada, Winnipeg, Manitoba, **2013**, pp. 15-119.
[10] A.D. Weeks, *J. Less Common Met.* **1961**, 3(6), 443-450.
[11] P. Kurttio, A. Auvinen, L. Salonen, H. Saha, J. Pekkanen, I. Mäkeläinen, S.B. Väisänen, I.M. Penttilä, H. Komulainen, *Environ. Health Perspect.* **2002**, 110, 337-342.
[12] W. Shin, J. Oh, S. Choung, B.W. Cho, K.S. Lee, U. Yun, N.C. Woo, H.K. Kim, *Chemosphere*, **2016**, 163, 108-115.
[13] J.Z. Byczkowski, A.P. Kulkarni, *Pro-oxidant biological effects of inorganic component of petroleum: vanadium and oxidative stress*, ManTEch-GEO-CENTERS Joint Venture, Dayton, OH, **1996**.
[14] J.M. Blake, S. Avasarala, K. Artyushkova, A.M.S. Ali, A.J. Brearley, C. Shuey, W.P. Robinson, C. Nez, S. Bill, J. Lewis, *Environ. Sci. Technol.* **2015**, 49, 8506-8514.
[15] T.K. Tokunaga, Y. Kim, J. Wan, L. Yang, *Environ. Sci. Technol.* **2012**, 46, 7471-7477.
[16] P.B. Barton Jr, *Am. Mineral.* **1958**, 43, 799-817.
[17] D.E. Appleman, H.T. Evans Jr, *Am. Mineral.* **1965**, 50, 825-842.
[18] F. Abraham, C. Dion, M. Saadi, *J. Mater. Chem.* 1993, 3, 459-463.
[19] F. Abraham, C. Dion, N. Tancret, M. Saadi, *Advanced Materials Research*, **1994**, 1-2, 511-520.
[20] D.C. Burciaga Valencia, M. Reyes Cortes, A. Reyes Rojas, M. Rentería Villalobos, H. Esparza Ponce, L. Fuentes Cobas, L. Fuentes Montero, M. Silva Saenz, E. Herrera Peraza, A. Muñoz, *Rev. Mex. Fis.* **2010**, 56, 75-81.
[21] P. Piret, J. Declercq, D. Wauters-Stoop, *Bull. Minéral.* **1980**, 103, 176-178.

MANUSCRIPT

[22] J. Borene, F. Cesbron, *Bull. Soc. Fr. Mineral. Cristallogr*. **1970**, 93, 426-432; J. Borene, F. Cesbron, *Bull. Soc. Fr. Mineral. Cristallogr*. **1971**, 94, 8-14.

[23] Y. Wang, X. Yin, Y. Zhao, Y. Gao, L. Chen, Z. Liu, D. Sheng, J. Diwu, Z. Chai, T.E. Albrecht-Schmitt, S. Wang, *Inorg. Chem*. **2015**, 54, 8449–8455; A. Mer, S. Obbade, P. Devaus, F. Abraham. *Cryst. Growth. Des*. **2019**, 19, 3305–3314.

[24] J. Plášil, *Z. Kristallogr*. **2017**, 232, 807-814.

[25] I. Duribreux, C. Dion, F. Abraham, M. Saadi, *J. Solid State Chem*. **1999**, 146, 258-265.

[26] A.M. Chippindale, S.J. Crennell, P.G. Dickens, *J. Mater. Chem*. **1993**, 3, 33-37; K. Beneke, U. Grosse-Brauckmann, G. Lagaly, A. Weiss, *Z. Naturforsch*. **1973**, B28, 408-415.

[27] C. Dion, S. Obbade, E. Raekelboom, F. Abraham, M. Saadi, *J. Solid State Chem*. **2000**, 155, 342-353.

[28] S. Obbade, C. Dion, L. Duvieubourg, M. Saadi, F. Abraham, *J. Solid State Chem*. **2003**, 173, 1-12.

[29] M. Saadi, C. Dion, F. Abraham, *J. Solid State Chem*. **2000**, 150, 72-80.

[30] A.M. Chippindale, P.G. Dickens, G.J. Flynn, G.P. Stuttard, *J. Mater. Chem*. **1995**, 5, 141-146.

[31] N. Tancret, S. Obbade, F. Abraham, *Eur. J. Solid State Inorg. Chem*. **1995**, 32, 195-207.

[32] S. Obbade, C. Dion, M. Saadi, F. Abraham, *J. Solid State Chem*. **2004**, 177, 1567-1574.

[33] S. Obbade, C. Dion, M. Saadi, S. Yagoubi, F. Abraham, *J. Solid State Chem*. **2004**, 177, 3909-3917.

[34] S. Chong, S.M. Aksenov, P.C. Burns, *Z. Kristallogr*. (submitted).

[35] F. Dal Bo, S.M. Aksenov, P.C. Burns, *J. Solid State Chem*. **2019**, 271, 126-134; F. Dal Bo, S.M. Aksenov, P.C. Burns, *Z. Kristallogr*. **2019**, 234, 228–238.

[36] C.A. Juillerat, V.V. Klepov, G. Morrison, K.A. Pace, H.-C. zur Loye, *Dalton Trans*. **2019**, 48, 3162–3181.

[37] R.L. Frost, J. Čejka, M.L. Weier, W.N. Martens, *J. Mol. Struct*. **2006**, 788, 115-125.

[38] R.L. Frost, J. Čejka, M.L. Weier, W. Martens, D.A. Henry, *Vib. Spectrosc*. **2005**, 39, 131-138.

[39] E.J. Baran, J.C. Pedregosa, P.J. Aymonino, *Monatsh. Chem*. **1975**, 106, 1085-1090.

[40] P. Schwendt, D. Joniaková, *Chem. Zvesti*. **1975**, 29, 381-386.

[41] a) I.L. Botto, E.J. Baran, M. Deliens, *Neues. Jb. Mineral., Mh*. **1989**, 1989, 212-218; b) R.L. Frost, K.L. Erickson, M.L. Weier, O. Carmody, *Spectrochim. Acta Part A*, **2005**, 61, 829-834.

[42] A.J. Lussier, R.A. Lopez, P.C. Burns, *Can. Mineral*. **2016**, 54, 177-283.

[43] P.C. Burns, M.L. Miller, R.C. Ewing, *Can. Mineral*. **1996**, 34, 845-880.

[44] V.A. Blatov, M. O'keeffe, D.M. Proserpio, *CrystEngComm*, **2010**, 12, 44-48.

[45] N.V. Chukanov, I.V. Pekov, *Rev. Mineral. Geochem*. **2005**, 57, 105-143.

[46] N.V. Chukanov, I.V. Pekov, R.K. Rastsvetaeva, *Russ. Chem. Rev*. 2004, 73, 205-223.

[47] S.M. Aksenov, N.V. Chukanov, I.V. Pekov, R.K. Rastsvetaeva, A.E. Hixon, *Micropor. Mesopor. Mater*. **2019**, 279, 128-132.

[48] S.M. Aksenov, S.A. Mackley, D.V. Deyneko, V.K. Taroev, V.L. Tauson, R.K. Rastsvetaeva, P.C. Burns, *Micropor. Mesopor. Mater*. **2019**, 284, 25-35.

[49] V.A. Blatov, A.P. Shevchenko, D.M. Proserpio, *Cryst. Growth Des*. **2014**, 14, 3576-3586.

[50] R.D. Shannon, Acta Crystallogr. 1976, A32, 751-767.

[51] G. Ferraris, E. Makovicky, S. Merlino, *Crystallography of modular materials*, OUP, Oxford, **2004**.

[52] R.K. Rastsvetaeva, S.M. Aksenov, *Crystallogr. Rep*. **2011**, 56, 910-934.

[53] J. Huang, A.W. Sleight, *Mater. Res. Bull*. **1992**, 27, 581-590; A.A. Vedernikov, Y.A. Velikodnyj, V.V. Ilyukhin, V.K. Trunov, *Dokl. Akad. Nauk SSSR*, **1982**, 263, 101-104.

[54] A. Mer, S. Obbade, M. Rivenet, C. Renard, F. Abraham, *J. Solid State Chem*, **2012**, 185, 180–186.

[55] S.V. Krivovichev, *Eur. J. Inorg. Chem*. **2010**, 2010, 2594-2603.

[56] K.A. Kubatko, P.C. Burns, *Am. Mineral*. **2006**, 91, 333-336.

[57] U. Kolitsch, G. Giester, *Mineral. Mag*. **2001**, 65, 717-724.

[58] E.M. Villa, J. Diwu, E.V. Alekseev, W. Depmeier, T.E. Albrecht-Schmitt, *Dalton Trans*. **2013**, 42, 9637-9644.

[59] F. Dal Bo, T. Kohlgruber, J.E. Szymanowski, S.M. Aksenov, P.C. Burns, *Cryst. Growth Des*. **2018**, 18, 7254-7258.

[60] S. Krivovichev, *Acta Crystallogr*. **2012**, A68, 393-398.

[61] S. Krivovichev, *Mineral. Mag*. **2013**, 77, 275-326.

[62] R.H. Blessing, *Acta Crystallogr*. **1995**, A51, 33-38.

[63] G. Sheldrick, *SADABS*, version 2014/4, **2014**.

[64] L. Palatinus, G. Chapuis, J. *Appl. Crystallogr*. **2007**, 40, 786-790.

[65] V. Petříček, M. Dušek, L. Palatinus, *Z. Kristallogr*. 2014, 229, 345-352.

[66] K. Momma, F. Izumi, *J. Appl. Crystallogr*. 2011, 44, 1272-1276.

[67] K. Brandenburg, *DIAMOND 3*; Crystal Impact GbR: Bonn, Germany, **2005**.

[68] P.C. Burns, R.C. Ewing, F.C. Hawthorne, *Can. Mineral*. 1997, 35, 1551-1570.

[69] N. Brese, M. O'keeffe, Acta Crystallogr. 1991, B47, 192-197.

WILEY-VCH

FULL PAPER

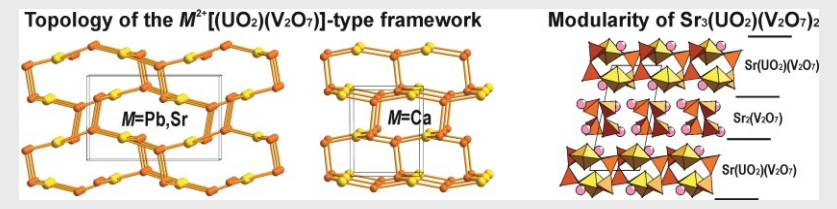

Uranyl vanadate compounds $M(UO_2)(V_2O_7)$ (M = Ca, Sr) and $Sr_3(UO_2)(V_2O_7)_2$, were synthesized by flux crystal growth, The topological polymorphism of the $[(UO_2)(V_2O_7)]$-type framework may be due to the differing ionic radii of the M^{2+} cations. Compound $Sr_3(UO_2)(V_2O_7)_2$ has a modular structure based on two different types of electroneutral layers: $[Sr(UO_2)(V_2O_7)]$ and $[Sr_2(V_2O_7)]$.

Uranyl vanadate compounds

*S. Chong, S.M. Aksenov, F. Dal Bo, S.N. Perry, F. Dimakopoulou, P.C. Burns**

1 – 7

Framework polymorphism and modular crystal structures of uranyl vanadates of divalent cations: synthesis and characterization of $M(UO_2)(V_2O_7)$ (M = Ca, Sr) and $Sr_3(UO_2)(V_2O_7)_2$

WILEY-VCH